

# Measurements of the three-dimensional shape of ice crystals in supercooled water

H. M. Singer\*

*Institute of Low Temperature Science, Hokkaido University, 060 Sapporo, Hokkaido, Japan*

(Received 30 May 2005; revised manuscript received 8 April 2006; published 24 May 2006)

Experimentally grown ice crystals from ultrapure supercooled water are imaged by means of Mach-Zehnder interferometry. By analyzing the fringe patterns the phase information and thus the three-dimensional shape of the ice crystals is recovered quantitatively. The integral parameters height of the basal plane, volume, and surface of the crystals are measured as a function of time and supercooling. It is found that all measured parameters follow a power law as a function of time and the exponents are found to be independent of the supercooling. The shape transition from the prismatic to the basal face along the main growth direction of the ice dendrites as a function of the distance from the tip is found to be a power law as well. Our findings support the validity of universal growth laws in pattern forming systems.

DOI: [10.1103/PhysRevE.73.051606](https://doi.org/10.1103/PhysRevE.73.051606)

PACS number(s): 81.10.-h, 64.70.Dv, 95.75.Mn

## I. INTRODUCTION

The formation of patterns in nature is ubiquitous [1,2]. Famous examples are cloud formation [3], bacterial colonies [4], and grain structures in metals [5] or rocks [6]. Apart from the technological importance of understanding the microstructure formation in metals in order to produce better casts, pattern formation, especially the most prominent dendritic morphology, is also of theoretical interest (e.g. [2]). Dendrites are a prototypical system evolving from homogeneous starting conditions into complex spatio-temporal patterns far from equilibrium.

Experiments on dendritic growth were mostly focused on systems with simple molecular structures (mostly fcc/bcc such as xenon [7,8], SCN or PVA [9]). In these systems fourfold symmetric 3D dendrites are found. Ice on the other hand was studied for a long time already e.g. [10,11] since it is relatively simple to perform experiments. Ice has a more complicated molecular structure; it crystallizes hexagonally and shows rough and therefore dendritic growth along the  $a$  axis and faceted growth along the  $c$  axis.

Most studies on dendritic growth even if the actual experiments were performed in 3D were concentrating on the 2D projection. Growth parameters such as growth velocity, tip radii, and side branch spacing have been determined from these projections and compared to theoretical models and computer simulations. These parameters describe only the behavior of the tip of the growing dendrite. Properties of the whole crystals can be described by integral parameters [7] such as fractal dimensions [8,12], contour length, projection area [7], or surface and volume in 3D [13,14].

Recently the research has tended to include 3D aspects of the dendritic crystals as well. First attempts to obtain a qualitative view of a growing ice dendrite were given by Shimada and Furukawa [15,16]. Teraoka *et al.* [17] report on the shape of the cross sections of ice crystals along the growth direction and find a square root dependence of the height as a function of the distance from the tip for different supercoolings. Singer and Bilgram have quantitatively reconstructed

the three-dimensional shape of experimentally grown xenon dendrites [13] and measured volume and surface as a function of the distance from the tip, time, and supercooling [14].

In this paper we report on the full three-dimensional reconstruction of growing ice crystals by means of Mach-Zehnder interferometry fringe pattern analysis and present for the first time results for the volume and surface growth of ice, which were inaccessible up to now.

## II. EXPERIMENTAL SETUP AND INTERFEROMETRIC 3D RECONSTRUCTION

Our experimental setup consists of a cylindrical growth cell ( $r=10$  mm and  $z=40$  mm) with optically flat glass plates, which is immersed in an ethanol heat bath with glass windows. The ice crystal is grown by the capillary injection technique [18]. Nucleation of the crystal occurs inside the capillary reaching into the growth vessel, thus enabling the crystal to grow freely in 3D once it reaches the opening of the capillary. The water is purified by means of deionization, distillation, and filtration. The resistivity was measured to be higher than  $10^7$   $\Omega$  cm. The *in situ* observation of the growing crystals is recorded by a video camera on an SVHS video with a resolution of  $720 \times 480$  pixels and finally digitized to 8-bit gray scale images on a computer. The temperature regime in which experiments were performed was  $\Delta T = T_m - T_{\text{exp}}$  and  $0.1$   $^\circ\text{C} \leq \Delta T \leq 1.0$   $^\circ\text{C}$  with  $T_m = 0$   $^\circ\text{C}$  the melting temperature and  $T_{\text{exp}}$  the temperature of the experiment.

The crystal is observed via a Mach-Zehnder interferometer. A dendrite grown at  $\Delta T = 0.5$   $^\circ\text{C}$  is shown in Fig. 1. If no crystal is present the split ray paths of the laser beam exhibit a regular interference fringe pattern. If a crystal is present the fringes change their intensity according to the height of the crystal. It is well known that the fringe pattern intensity is then given by

$$I(x,y) = a(x,y) + b(x,y)\cos[2\pi f_0 x + \Psi(x,y)], \quad (1)$$

where  $a(x,y)$  is a slowly changing background intensity,  $b(x,y)$  is the contrast component also varying slowly,  $f_0$  is the carrier frequency, and  $\Psi(x,y)$  corresponds to the phase

\*Electronic address: [hsinger@solid.phys.ethz.ch](mailto:hsinger@solid.phys.ethz.ch)

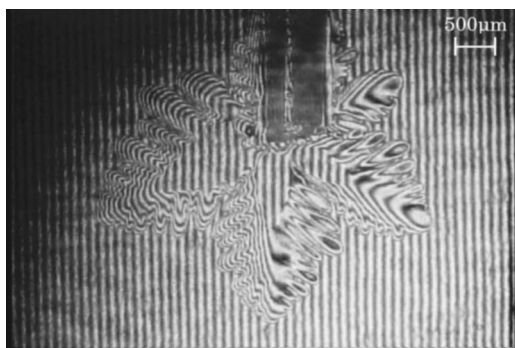


FIG. 1. Growing ice dendrite in supercooled water with  $\Delta T=0.5$  °C observed via a Mach-Zehnder interferometer. From the interference fringes the height distribution of the crystal can be calculated.

distortion introduced by the crystal. The height or thickness distribution of the growing crystal is given as

$$d(x,y) = \lambda\Psi(x,y)/[2\pi|n_i - n_w|] \quad (2)$$

with the wavelength  $\lambda=632.8$  nm and the refractive indices of ice  $n_i=1.3078$  and water  $n_w=1.3327$  at 0 °C, respectively.

In earlier approaches to obtain the three-dimensional shape of growing ice crystals [15,16] a carrier frequency  $f_0$  was chosen so that the distance between neighboring interference fringes was large compared to the ice crystal dimension. Then the fringes on the ice crystal could be considered in an raw approximation as iso-height lines of the crystals and the height difference between two successive fringes in

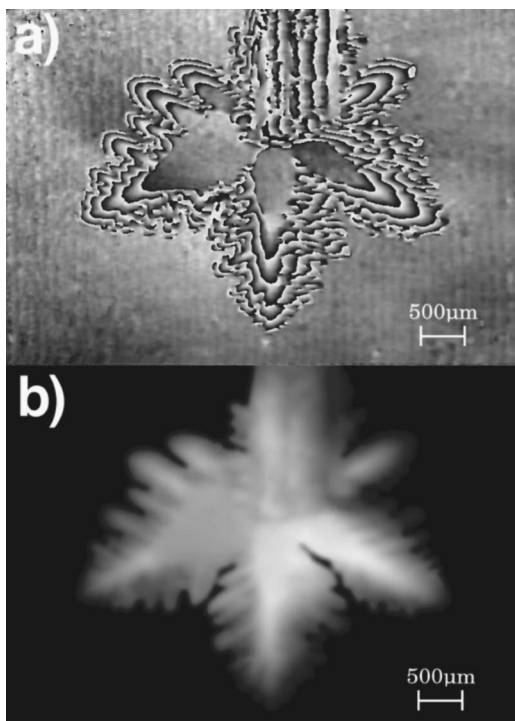


FIG. 2. (a) Wrapped phase data after subtracting the interference fringes phase without crystal. (b) Unwrapped phase data. Unwrapping was performed by solving Eq. (4).

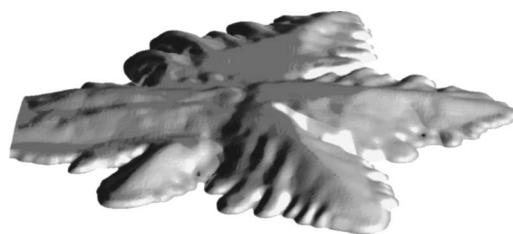


FIG. 3. Three-dimensional representation of the unwrapped phase data of the growing ice crystal.

the crystal was calculated to be  $25.4$   $\mu\text{m}$ . Although this approach gave first qualitative insights on the 3D shape it did not reveal enough details to reconstruct the crystal fully as a function of time.

We have reconstructed the three-dimensional shape of the crystal in a more general way—independently of the carrier frequency  $f_0$ . The method is also used in Synthetic Aperture Radar Imagery (SAR) for geographical height measurements from planes or satellites. The key point is to reconstruct the phase profile  $\Psi(x,y)$ . The wrapped phase profile [as all the  $\Psi$  values are in the interval  $-\pi \leq \mathcal{W}(\Psi) < \pi$ , where  $\mathcal{W}(\cdot)$  denotes the wrapping operator] is determined by Fourier methods: The two-dimensional Fourier transform of Eq. (1) of the intensity profile with and without crystal are calculated. By back transforming the first order peaks only and subtracting the results from each other the wrapped phase profile  $\mathcal{W}(\Psi)$  is obtained. The wrapped phase plot is shown in Fig. 2(a). In order to calculate the actual phase  $\Psi$  from  $\mathcal{W}(\Psi)$  many phase unwrapping (PU) algorithms have been proposed (e.g., [19–21]). As our data shows quite a large amount of residual points (typically around 12%–15%) path following PU algorithms could not be used. On the other hand Fourier based methods, which minimize an error function (especially the unweighted ones) tend to underestimate the actual height of the data. We have thus chosen a recently proposed algorithm [22], which is very robust and does not use a minimization function; additionally as it calculates the Laplacians by Fourier methods the influence of residues is less noticeable. The basic idea is that

$$\Psi(x,y) = \mathcal{W}(\Psi) + 2\pi n(x,y), \quad (3)$$

where  $n(x,y)$  indicates an integer field of multiples of  $2\pi$ . In order to solve this problem it can be shown [22] that  $\nabla^2\Psi$  can be expressed as a function of  $\nabla^2\mathcal{W}(\Psi)$ :  $\nabla^2\Psi = \cos \mathcal{W}(\Psi)\nabla^2(\sin \mathcal{W}(\Psi)) + \sin \mathcal{W}(\Psi)\nabla^2(\cos \mathcal{W}(\Psi))$ . By rearranging Eq. (3) we find

$$n(x,y) = \frac{1}{2\pi}\nabla^{-2}(\nabla^2\Psi - \nabla^2\mathcal{W}(\Psi)), \quad (4)$$

where  $\nabla^2$  and  $\nabla^{-2}$  are the 2D Laplacian and inverse Laplacian, respectively. We can now solve Eq. (4) by Fourier methods and round the found field  $n(x,y)$  to the nearest integer values. The found result of the phase unwrapped data of Fig. 2(a) is shown in Fig. 2(b). Finally the background of Fig. 2(b) is removed by subtracting the background average from the image and extracting only the heights, which are in the mask given by the contour of the crystal. A three-

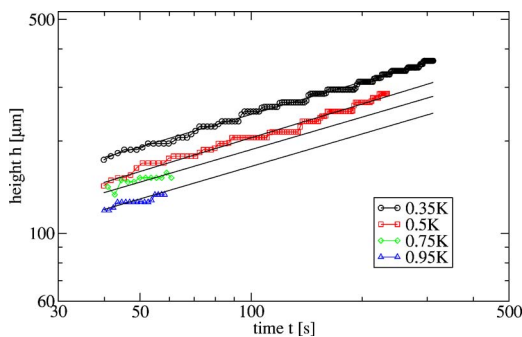


FIG. 4. (Color online) Height of the basal plane as a function of time for different supercoolings.

dimensional view of the reconstructed crystal is shown in Fig. 3.

### III. RESULTS

We have measured the height of the basal plane as a function of the time in the interferometric observations of the ice crystals for different supercoolings. The measurement was performed as follows. A reference interference fringe outside the crystal and a fringe on the basal plane were chosen. When the height of the basal plane is increasing, the fringe intensity is changing as well. A uniform fringe shift is observed on areas with equal heights. By extracting (1+1) space-time plots from the data it was possible to calculate the distance between the two selected fringes as a function of time. This distance is proportional to the height of the crystal. The results of the measurements are given in Fig. 4. We find that the height of the basal plane increases as a power law  $h(t) = h_0(\Delta T)t^\alpha$ , where  $h_0$  is a parameter depending on supercooling. The exponent  $\alpha$  was found to be  $\alpha = 0.35 \pm 0.02$  independent of the supercooling. This is in good agreement with the findings of Teraoka *et al.* [17] who found that the growth velocity of the facet decays as  $v_c(t) = v_0 \cdot t^{-0.67}$ .

With the phase unwrapping method explained above we have calculated the 3D shape of the temporal evolution of crystals for different supercoolings. The results for the volume and the surface of the crystals are given in

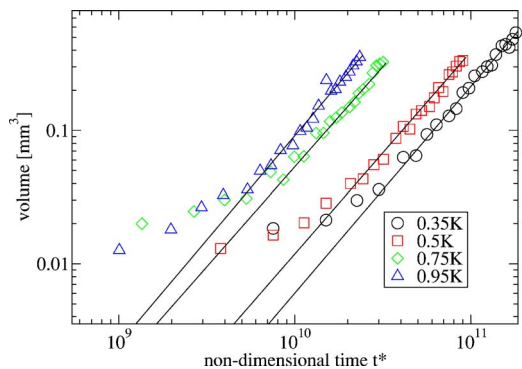


FIG. 5. (Color online) Volume of the dendrite as a function of the time for different supercoolings.

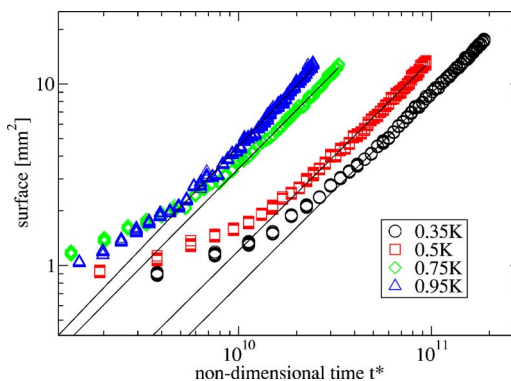


FIG. 6. (Color online) Surface of the dendrite as a function of time for different supercoolings.

Figs. 5 and 6, respectively. The time was nondimensionalized  $t^* = v(\Delta)t/d_0$  with  $v(\Delta)$  the supercooling dependent tip velocity and  $d_0 = 2.88 \times 10^{-8}$  cm the capillary length of water. The length scale  $d_0$  was chosen for nondimensionalization since there is no unique other length scale available as in the 3D crystal now two different tip radii occur (in the  $x$ - $y$  plane, along the  $a$  axis  $\rho_a$  and perpendicular in the  $x$ - $z$  plane  $\rho_c$ ), which behave entirely different upon the change of supercooling [15]. In order to not favor one supercooling dependent scale over the other the constant value of  $d_0$  provided the necessary conversion. As  $d_0$  is very small compared to typical lengths of the crystal, this leads to big numbers in the nondimensional time  $t^*$ , as can be seen in Figs. 5 and 6.

We have found that both volume and surface obey a power law and that the exponents are independent of the supercooling. We find therefore that  $V(t) = V_0(\Delta T)t^\gamma$  and  $S(t) = S_0(\Delta T)t^\beta$  with the volume exponent  $\gamma = 1.52 \pm 0.08$  and the surface exponent  $\beta = 1.07 \pm 0.02$ .

In Fig. 7 the cross sections along the main growth axis rescaled by the respective generalized tip radius [23] are shown. It can be clearly seen that the shape is identical for different supercoolings. A fit of the data shows that the measurements of Teraoka *et al.* [17] fitting the cross sections along the axis with a parabola (exponent 0.5) must be considered as a crude approximation of the real power

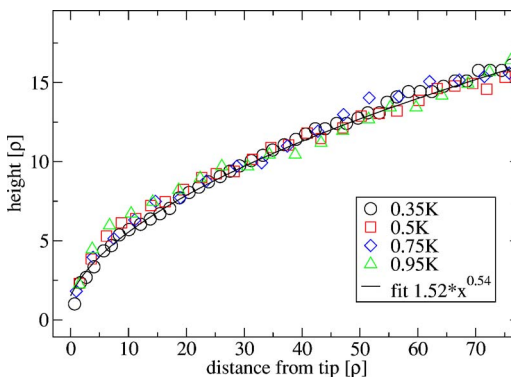


FIG. 7. (Color online) Cross sections along the main axis of growth in units of the generalized tip radius [23]. The shape is independent of the supercooling.

law. More accurately the fit is described with the exponent  $\delta=0.54\pm 0.02$  as a function of the distance from the tip, this means that the shape is not a parabola but a power law with the exponent  $1.85\pm 0.04$ .

#### IV. DISCUSSION AND CONCLUSION

We have found a power law dependence on the time for all measured parameters height of the basal plane, volume, and surface. The exponents are independent of the supercooling. In particular it is interesting to note that despite the high anisotropy of the crystal, which includes faceting in one growth direction the growth exponents found, are identical to the ones, which would be expected for the growth of the completely isotropic case of a sphere in diffusional growth, growing with  $\sqrt{t}$  per dimension leading to  $t^{1.5}$  in 3D. The results indicate that only the diffusion is rate limiting, despite the clear faceting along the  $c$  axis of the ice crystal.

In [15] it was shown that the tip velocity along the  $a$  axis behaves according to the theoretical expectations of the L-MK-theory [24]. At the same time however it was shown that the stability constants  $\sigma_i^* = Dd_o / (v\rho_i^2)$ ,  $i=a,c$  behave completely different for rough and faceted growth. While the rough growth showed a constant  $\sigma_a^*$  for  $\rho_a$ , the stability constant  $\sigma_c^*$  calculated from  $\rho_c$  was strongly dependent on the supercooling. Combining these results with the results found for the volume solidification rate  $dV/dt = 1.52 * V(\Delta)t^{0.52}$  in this paper it follows that the total solidification rate for the

whole crystal and therefore also the stability constant is dependent on the supercooling. This is also in accordance with [25] stating about the L-MK theory in highly anisotropic systems (p. 20): “It seems to me that the present form of the theory cannot be adequate to describe so highly anisotropic a system, and that, in particular, anisotropic attachment kinetics must be included in both the steady state calculation and the stability analysis.”

The cross sections along the growth axis exhibit a supercooling independent growth shape when rescaled by the respective tip radius and can be described by a power law as a function of the distance from the tip.

The results found from our measurements suggest that in spite of the complex growth shapes exhibited in pattern forming systems like ice, xenon or SCN integral parameters of these substances such as volume or surface, which take also into account the nonlinear interaction between competing side branches are (i) a reliable method to reproducibly measure experimental data and (ii) the growth of the crystals can be described by very simple growth laws. The independence of the exponents from the driving force of the supercooling indicates that the growth process is universal and the exponents are only dependent on material properties.

#### ACKNOWLEDGMENTS

The author thanks Professor Y. Furukawa for the use of the experimental setup. This work was supported by a grant of the Japanese Society for the Promotion of Science (JSPS).

- 
- [1] *Branching in Nature*, edited by V. Fleury, J. F. Gouyet, and M. Leonetti (Springer, Berlin, 2001).
- [2] J. S. Langer, in *Chance and Matter: Les Houches, Sessions XLVI, 1986*, edited by J. Souletie, J. Vannimenus, and R. Stora (Elsevier Science, Amsterdam, 1987), pp. 629–711.
- [3] J. Feder, *Fractals* (Plenum, New York, 1988).
- [4] T. Matsuyama and M. Matsushita, *Crit. Rev. Microbiol.* **19**, 117 (1993).
- [5] D. M. Stefanescu, *Science and Engineering of Casting Solidification* (Kluwer Academic, New York, 2002).
- [6] S. S. Augustithis, *Atlas of the Textural Patterns of Ore Minerals and Metallogenic Processes* (de Gruyter, Berlin, 1995).
- [7] E. Hürlimann, R. Trittbach, U. Bisang, and J. H. Bilgram, *Phys. Rev. A* **46**, 6579 (1992).
- [8] U. Bisang and J. H. Bilgram, *Phys. Rev. E* **54**, 5309 (1996).
- [9] M. E. Glicksman and N. B. Singh, *J. Cryst. Growth* **98**, 277 (1989).
- [10] S. H. Tirmizi and W. N. Gill, *J. Cryst. Growth* **85**, 488 (1987).
- [11] K. K. Koo, R. Ananth, and W. N. Gill, *Phys. Rev. A* **44**, 3782 (1991).
- [12] H. M. Singer and J. H. Bilgram, *Physica D* (in press).
- [13] H. M. Singer and J. H. Bilgram, *Europhys. Lett.* **68**, 240 (2004).
- [14] H. M. Singer and J. H. Bilgram, *Physics Rev. Lett.* (unpublished).
- [15] Y. Furukawa and W. Shimada, *J. Cryst. Growth* **128**, 234 (1993).
- [16] W. Shimada and Y. Furukawa, *J. Phys. Chem.* **101**, 6171 (1993).
- [17] Y. Teraoka, A. Saito, and S. Okawa, *Int. J. Refrig.* **27**, 242 (2004).
- [18] M. E. Glicksman, R. J. Schaefer, and J. D. Ayers, *Metall. Trans. A* **7A**, 1747 (1976).
- [19] D. C. Gighlia and A. Romero, *J. Opt. Soc. Am. A* **11**, 107 (1994).
- [20] M. D. Pritt, *IEEE Trans. Geosci. Remote Sens.* **GE-34**, 728 (1996).
- [21] T. J. Flynn, *J. Opt. Soc. Am. A* **14**, 2692 (1997).
- [22] M. A. Schofield and Y. Zhu, *Opt. Lett.* **28**, 1194 (2003).
- [23] H. M. Singer and J. H. Bilgram, *Phys. Rev. E* **69**, 032601 (2004).
- [24] J. S. Langer and H. Müller-Krumbhaar, *Acta Metall.* **26**, 1681 (1978).
- [25] J. S. Langer, *Rev. Mod. Phys.* **52**, 1 (1980).